Cell, Vol. 106, 563–573, September 7, 2001, Copyright ©2001 by Cell Press

FOXC2 Is a Winged Helix Gene that Counteracts Obesity, Hypertriglyceridemia, and Diet-Induced Insulin Resistance

Anna Cederberg,[1] Line M. Grønning,[3] Bo Ahrén,[4] Kjetil Taskén,[3] Peter Carlsson[2] and Sven Enerbäck[1,5]
[1]Medical Genetics, Department of Medical Biochemistry
[2]Department of Molecular Biology
Göteborg University
Box 440
SE-405 30 Göteborg
Sweden
[3]Institute of Medical Biochemistry
University of Oslo
N-0317 Oslo
Norway
[4]Department of Medicine
Lund University
Malmö University Hospital
SE-205 02 Malmö
Sweden

Summary

Obesity, hyperlipidemia, and insulin resistance are common forerunners of type 2 diabetes mellitus. We have identified the human winged helix/forkhead transcription factor gene *FOXC2* as a key regulator of adipocyte metabolism. Increased *FOXC2* expression, in adipocytes, has a pleiotropic effect on gene expression, which leads to a lean and insulin sensitive phenotype. *FOXC2* affects adipocyte metabolism by increasing the sensitivity of the β-adrenergic-cAMP-protein kinase A (PKA) signaling pathway through alteration of adipocyte PKA holoenzyme composition. Increased *FOXC2* levels, induced by high fat diet, seem to counteract most of the symptoms associated with obesity, including hypertriglyceridemia and diet-induced insulin resistance—a likely consequence hereof would be protection against type 2 diabetes.

Introduction

High calorie diet and low physical activity are important etiological factors for type 2 diabetes (also known as noninsulin dependent diabetes mellitus, NIDDM). The majority of such patients are obese. It has been predicted that by the year 2020, some 250 million people world-wide will suffer from type 2 diabetes. Since this disease is a major risk factor for ischemic heart disease and a common cause to renal failure, midlife blindness, and lower extremity amputations, this threatening epidemic will have profound public health implications (O'Rahilly, 1997; Zimmet and Alberti, 1997). One major problem in the treatment of type 2 diabetes is to increase insulin sensitivity without promoting adipocyte differentiation (e.g., thiazolidindiones) and/or enlarge triglyceride stores (e.g., insulin) which has the potential of counteracting the initial benefits of such treatments, since more and larger adipocytes will increase insulin resistance (Abbott and Foley, 1987). An ideal therapy should not only increase insulin sensitivity but also provide means by which excess energy could be dissipated. A great deal of interest has focused on adaptive thermogenesis as a physiological defense against obesity, hyperlipidemia, and diabetes (Hamann et al., 1996). Adaptive thermogenesis occurs to a large extent in mitochondria of skeletal muscle and brown adipose tissue (BAT). In BAT, ucp1 (uncoupling protein-1) has the ability to dissipate energy through uncoupling of oxidative phosphorylation which, instead of generating ATP, will produce heat. There are great individual differences in how a caloric overload is handled. Some people store most of the energy in their white adipose tissue (WAT), whereas others dissipate much of it through altered energy expenditure including adaptive thermogenesis (Bouchard et al., 1990; Levine et al., 1999). It is likely that these differences can be explained by genetic factors.

Several studies using genetically modified mice have made valuable contributions to our understanding of adipocyte metabolism, obesity, and insulin resistance. Most of these mice have specific and well-defined alterations in adipocyte function affecting insulin action (Shepherd et al., 1993), differentiation (Moitra et al., 1998; Shimomura et al., 1998), metabolism (Osuga et al., 2000), sensitivity to adrenergic stimuli (Susulic et al., 1995), or intracellular signaling pathways (Cummings et al., 1996). We show that in mice overexpressing *FOXC2*, in WAT and BAT, the intraabdominal WAT depot is reduced and has acquired a brown fat-like histology whereas interscapular BAT is hypertrophic. Increased *FOXC2* expression has a pleiotropic effect on gene expression in BAT and WAT. There is an induction of the BAT-specific gene *ucp1* in the intraabdominal WAT depot. We also demonstrate a change in steady-state levels of several WAT and BAT derived mRNAs, encoding genes of importance for adipocyte: (1) insulin action, (2) differentiation, (3) metabolism, (4) sensitivity to adrenergic stimuli, and (5) intracellular signaling. The nature of these *FOXC2*-generated responses is consistent with protection against obesity and related symptoms such as diet induced insulin resistance. Furthermore, in wt (wild-type) mice, we demonstrate that *Foxc2* mRNA levels are upregulated by high fat diet and that mice with targeted disruption of one *Foxc2* allele have a decreased interscapular BAT cell mass. These observations support the view of *Foxc2* as an important regulator of adipocyte metabolism with the ability to alter metabolic efficiency in response to dietary changes.

Results

FOXC2 Is Expressed in WAT and BAT during Postnatal Life

We have provided evidence for the existence of a winged helix/forkhead gene expressed in adipocytes

[5]Correspondence: sven.enerback@medgen.gu.se

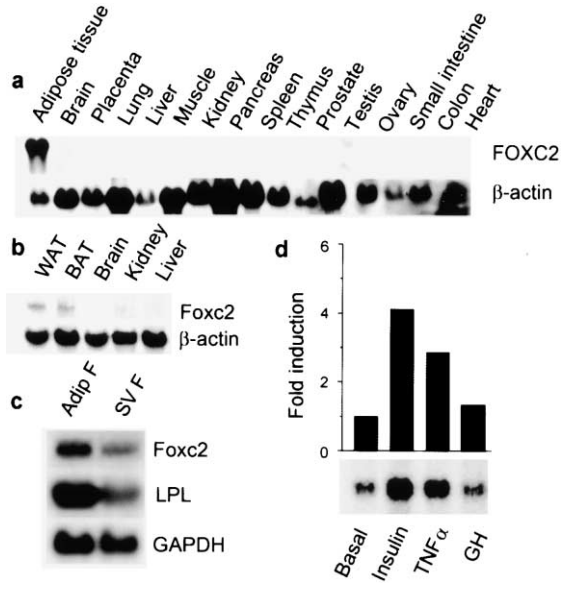

Figure 1. Northern Blot Analysis

Adult human tissues (a) and wt adult mouse tissues (b). The blots were analyzed with probes specific (with no cross-reactivity) for *FOXC2* (human) and *Foxc2* (mouse), respectively. The experiments were carried out with 20 μg of total RNA/lane using β-actin as an internal control. Mouse adipose tissue (c) was treated with collagenase (see under "Experimental Procedures"); RNA from the adipocyte fraction (Adip F) and the stroma/vascular fraction (SV F) were used and probed for *Foxc2*, *LPL* (adipocyte marker), and *GAPDH* (control). In (d), differentiated murine adipocytes (3T3-L1) were stimulated for 2 hr with insulin (10 μg/ml), TNFα (50 ng/ml), growth hormone (GH;100 ng/ml) or left untreated (Basal). Northern blot analysis was performed and the *Foxc2* mRNA signal was assessed by β-scintillation counting in a dot-matrix β-counter. Image shows counts over the filter plotted in gray-scale intensity. Bars above the Northern blot represent actual cpm over mean cpm of controls subtracted of background cpm given as "fold induction."

(Enerback et al., 1992). To find this gene, we screened a human adipocyte cDNA library; two overlapping clones representing the human homolog of the mouse gene *Foxc2* were isolated. Mice lacking *Foxc2* have cranofacial, vertebral, and aortic arch malformations. Since such mice die embryonically or perinatally (Iida et al., 1997; Winnier et al., 1997), little is known about the function of *Foxc2* during postnatal life. Northern blot with mRNA from *Homo* (Figure 1a), shows that *FOXC2* is exclusively expressed in WAT. This human gene is also known as *MFH1* (mesenchyme forkhead-1) or *FKHL14*; the mouse homolog is known as *Foxc2* or *mfh1*. In this paper, we follow a recently adopted nomenclature and use the gene names *FOXC2* and *Foxc2* to designate the human and mouse genes, respectively. Using mouse mRNA, we demonstrate expression of *Foxc2* in both WAT and BAT (Figure 1b). A more sensitive assay for transcript detection, such as RT-PCR, shows low levels of *Foxc2* mRNA in striated muscle from adult mice (not shown). In a Northern blot experiment using RNA from collagenase prepared adipocytes, we could demonstrate that *Foxc2* expression is highest in the adipocyte fraction with a lower level of expression in stroma/vascular cells (Figure 1c). When adipocytes are treated with insulin or TNFα, *Foxc2* mRNA levels increase, whereas growth hormone does not appear to regulate *Foxc2* (Figure 1d). The fact that two major regulators of glucose/adipocyte metabolism—insulin and TNFα—regulate *Foxc2* in vitro made us interested in the role of *Foxc2* in vivo.

FOXC2 Regulates Adipose Tissue Distribution and Morphology

We made a DNA construct in which the adipose-specific aP2 (Coe et al., 1999) enhancer/promoter, known to promote transcription in BAT and WAT in vivo (Ross et al., 1990), was fused to a cDNA encoding *FOXC2*. Mice transgenic for this construct appear normal in terms of general behavior and reproduction. Tg (transgenic) mice have distinctly enlarged bilobed interscapular BAT depots (Figures 2a and 2b), whereas the intraabdominal WAT depot is clearly reduced (Figures 2c and 2d). Analyses were performed on *FOXC2* tg-A mice with wt littermates as controls, mice were approximately 4–6 months of age and fed ad libitum. The intraabdominal WAT from tg mice has a brownish color, in contrast to the corresponding WAT in non-tg animals, which is light yellow (Figures 2e and 2f). Histological examination of these fat depots demonstrates an increased size of the lipid droplets in BAT from tg mice (Figures 2g and 2h). The intraabdominal WAT in tg animals has a clearly reduced cell size and regions of small cells with multilocular fat droplets (Figures 2i and 2j). In a cold adaptation experiment (4°C, 24 hr), tg mice display a clear reduction in size and number of triglyceride droplets in BAT (Figures 2k–2n). This indicates that changes in gene expression, induced by the transgene, will allow a net accumulation of triglyceride at room temperature (22°C), whereas these triglycerides are metabolized at 4°C.

We selected three independent founder lines, tg-A, tg-B, and tg-C with tg-A having the highest, tg-B the lowest, and tg-C an intermediate level of *FOXC2* expression in WAT (Figure 4a). There is a dose-response relation between the expression level of the transgene and reduction in the relative weight of the intraabdominal WAT depot (Figure 3a). A similar dose-response exists for the weight ratios of intraabdominal WAT to interscapular BAT (Figure 3b). The relative weight of the interscapular BAT depot is increased in tg animals but does not exhibit any dose-response pattern (Figure 3a), which is in accordance with the fact that there is no difference between tg-A, tg-B, and tg-C in expression of the transgene in BAT (Figure 4a). Livers from wt and tg-A mice appear normal in terms of gross morphology, weight, and lipid content (not shown).

Increased FOXC2 Expression Has a Pleiotropic Effect on Gene Expression

Steady-state levels of 21 different mRNAs were examined in WAT and BAT (Figure 4b). Interestingly, there is a dose-dependent induction of the BAT-specific marker gene *ucp1* in WAT (Figure 4b). The tg line with the highest level of *FOXC2* expression (tg-A) has the most prominent *ucp1* induction (Figure 4b). The expression of *ucp2* is reciprocally regulated as compared with *ucp1*, and this type of regulation has previously been reported in mice lacking *ucp1* (Enerback et al., 1997). Genes associated with mitochondrial function and biogenesis such as

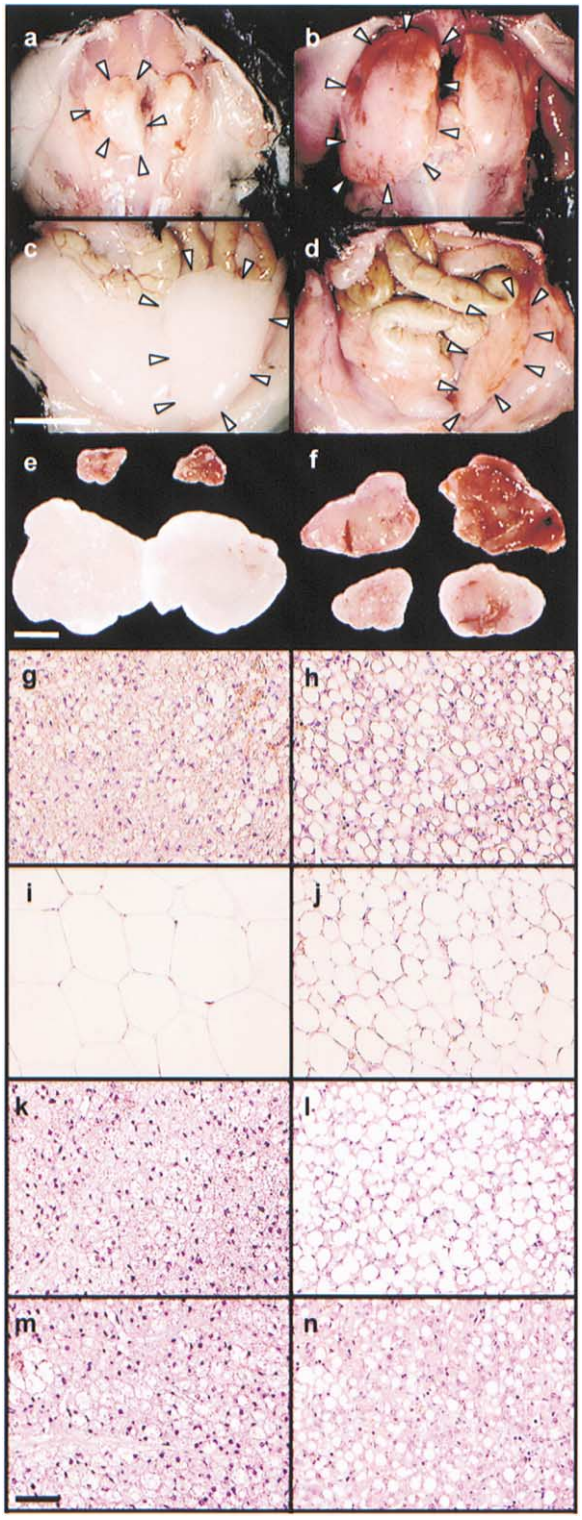

Figure 2. Morphology and Histology of WAT and BAT from Wild-type (a, c, e, g, i, k, and m) and *FOXC2* tg-A (b, d, f, h, j, l, and n)

An exposed dorsal view of the bilobed interscapular brown fat (white arrows) (a and b). A ventral view of the intraabdominal white fat pads (white arrows) in tg (d) and wt (c) mouse. A comparison of interscapular brown fat pads and intraabdominal white fat pads from wt (e) and tg (f) mice. BAT at the top and WAT at the bottom. Histological sections of interscapular brown fat from wt (g) and tg (h) mouse. Sections from intraabdominal WAT depots in wt (i) and tg (j) mouse. In a cold adaptation experiment, mice were kept at either room temperature (RT) or at 4°C for 24 hr, sections from wt ([k], RT; [m], 4°C) and tg ([l], RT; [n], 4°C) BAT. Scale bar for (a)–(d), depicted in (c) equals 5 mm, scale bar for (e) and (f), depicted in (e) equals 5 mm, scale bar for (g)–(n), depicted in (m) equals 100 μm.

coxII (cytochrome c-oxidase subunit II), encoded by the mitochondrial genome, and *pgc1* (PPARγ coactivator-1) (Wu et al., 1999a) are upregulated in WAT (Figure 4b). The induction of *ucp1* in WAT and the altered WAT morphology (Figures 2i and 2j) indicates a transition toward BAT-like properties of the intraabdominal WAT depot. mRNA levels for $\beta_{1\text{-}3}$-AR ($\beta_{1\text{-}3}$-adrenergic receptors) are all upregulated in WAT. The most prominent induction is in mRNA levels for β_3-AR in WAT. This is indicative of increased sensitivity to adrenergic stimuli.

Transcription factors known to promote adipocyte differentiation such as *C/EBP*α (CCAAT-box enhancer binding protein-α) (Lin and Lane, 1994), *PPAR*γ (peroxisome proliferator-activated receptor-γ) (Tontonoz et al., 1994), and *ADD1/SREBP1* (adipocyte determination and differentiation-dependent factor-1/sterol regulatory element binding protein-1) (Kim and Spiegelman, 1996) are upregulated in tg WAT (Figure 4b). Even though the WAT depot is decreased in size in tg animals, the adipocyte differentiation per se appears to be stimulated. Both *aP2* (Coe et al., 1999) and *adipsin* (Murray et al., 1999) are upregulated (Figure 4b). *Adipsin* is induced in both WAT and BAT in a dose-dependent manner in relation to transgene expression. The level of *LPL* (lipoprotein lipase) mRNA is only slightly upregulated, whereas the intracellular and PKA phosphorylation activated lipase—*HSL* (hormone sensitive lipase)—is clearly induced in WAT. *Leptin* mRNA levels are reciprocally downregulated in relation to expression levels of the transgene and, in tg BAT, no *leptin* mRNA can be identified (Figure 4b). mRNA levels of four genes, representing the insulin pathway, are induced: *IR* (the insulin receptor), *IRS1*, *IRS2* (insulin receptor substrate-1 and -2), and *GLUT4* (insulin-responsive glucose transporter-4). This is consistent with an increased insulin sensitivity and triglyceride synthesis in adipocytes. The induced level of *HSL* mRNA together with increased sensitivity to β-adrenergic stimuli is compatible with an increased intracellular capability to induce and maintain lipolysis. This process can provide FFA as a source of energy for *ucp1*-induced heat production. Upregulation of *PPAR*α (peroxisome proliferator-activated receptor-α) in WAT (Figure 4b) suggests an increase in fatty acid β-oxidation. This is consistent with low levels of FFA and a lean phenotype (Figures 2 and 3).

FOXC2 Regulates Body Composition, Serum Lipids, and Insulin Sensitivity

There is a decrease from 30% total lipids in carcasses of wt mice as compared with 10% in tg mice ($p < 0.001$; Figure 3c). A significant reduction in serum triglyceride levels of 57% ($p < 0.004$; Figure 3d) is observed, whereas no significant change in serum cholesterol can be detected (Figure 3e). FFAs are lowered from 0.92 meq/l to 0.63 meq/l in tg animals ($p < 0.02$; Figure 3f). Plasma

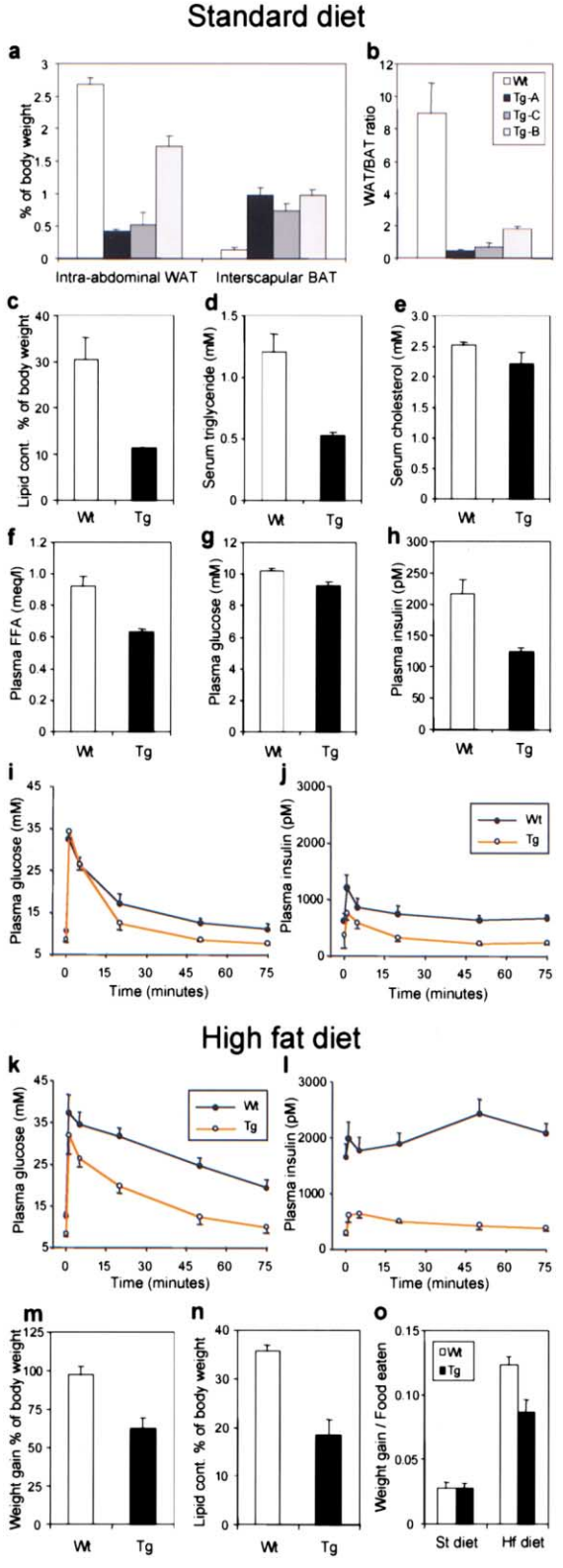

Figure 3. Weight Comparison of BAT and WAT Depots

In (a), weights of intraabdominal WAT and interscapular BAT depots from tg mice (founder lines A, B, and C) are compared to that of wt mice. Ratios between weights of intraabdominal WAT to interscapular BAT for wt and tg founder lines A, B, and C (b). Values are means ± SEM, n = 4 in each group. Metabolic profile, on standard diet (c–h).

glucose is down by 10% ($p < 0.01$; Figure 3g) and plasma insulin levels are reduced by 43% ($p < 0.001$; Figure 3h). In tg mice, on a high fat diet, the weight gain is 28% lower ($p < 0.01$; Figure 3m) as compared with wt. Although lipid content in tg and wt mice are increased after a high fat diet, tg mice still resist lipid accumulation to the same degree as is the case for wt littermates—a 49% decrease in tg mice as compared with wt ($p < 0.0001$; Figure 3n). On a standard diet (4.0% fat), tg and wt mice display no signs of differences in metabolic efficiency as judged by the ratio between weight gain and weight of food eaten (Figure 3o). They do, however, display a different body composition (Figure 3c). When fed a high fat diet (35.9% fat), tg mice appear less efficient in their metabolism, since they need to eat more for each gram of increase in body weight (a reduction of 30%, $p < 0.01$; Figure 3o). We would like to point out that the amount of food eaten, both on a standard and high fat diet, is the same for tg and wt mice. Thus, the difference seen on a high fat diet is derived from a less efficient metabolism in tg mice—not allowing triglycerides to accumulate to the same extent as in wt littermates. This is reflected by a decreased weight gain for mice on a high fat diet (Figure 3o), and a leaner body composition in tg mice regardless of type of diet (Figures 3c and 3n). These findings are interesting since they suggest that metabolic efficiency in *FOXC2* tg mice can be regulated in response to food composition. There are no significant differences in serum glucagon levels, nor have we observed any significant gender differences.

In an intravenous glucose tolerance test, plasma glucose for tg mice on standard diet is significantly lower at 0, 20, and 75 min ($p < 0.05$), and at 50 min ($p < 0.02$; Figure 3i). The insulin curve exhibits lower insulin levels for tg mice (Figure 3j) at 0 min ($p < 0.02$), at 1, 5, and 20 min ($p < 0.05$), and at 50 and 75 min ($p < 0.001$). On high fat diet, the difference is much more pronounced (Figures 3k and 3l). Glucose levels are lower in tg mice

Analyses were performed on *FOXC2* tg-A mice with wt littermates as controls, mice were approximately 4–6 months of age and fed adlibitum, if not otherwise indicated, n = 4 for each group, and values are means ± SEM. (c) Total body lipid content was analyzed as total lipid content of carcasses (see under "Experimental Procedures"). (d) Serum triglyceride. (e) Serum cholesterol. (f) Plasma free fatty acids (FFA). (g) Nonfasting plasma glucose. n = 20 in each group. (h) Plasma insulin. Analysis was performed on the same animals as in (g). Intravenous glucose tolerance test. Wt and *FOXC2* tg-A mice were fed a standrad (i and j) or high fat (k and l) diet for 14 weeks (for details, see "Experimental Procedures"). After intravenous (iv) injection of glucose (1 g/kg), blood samples were drawn immediately before and at 1, 5, 20, 50, and 75 min for analysis of glucose and insulin. Plasma glucose levels from wt and tg mice both on a standard i (tg, n = 8; wt, n = 9) and high fat diet k (tg, n = 5; wt, n = 6). Plasma insulin from wt and tg mice both on a standard diet (j) and a high fat diet (l). Diet-induced weight gains (high fat diet) in *FOXC2* tg (n = 7) mice as compared with wt (n = 9; [m]). Body lipid content after a high fat diet (tg, n = 6; wt, n = 4) in (n). The weight gain to grams of food eaten ratio was calculated for wt (n = 10) and tg (n = 9) mice on a standard (St) diet as well as for mice on a high fat (Hf) diet (tg, n = 7; wt, n = 9) (o). No gender differences were observed. For details concerning the diets and magnitude of changes observed see "Experimental Procedures" and corresponding text sections.

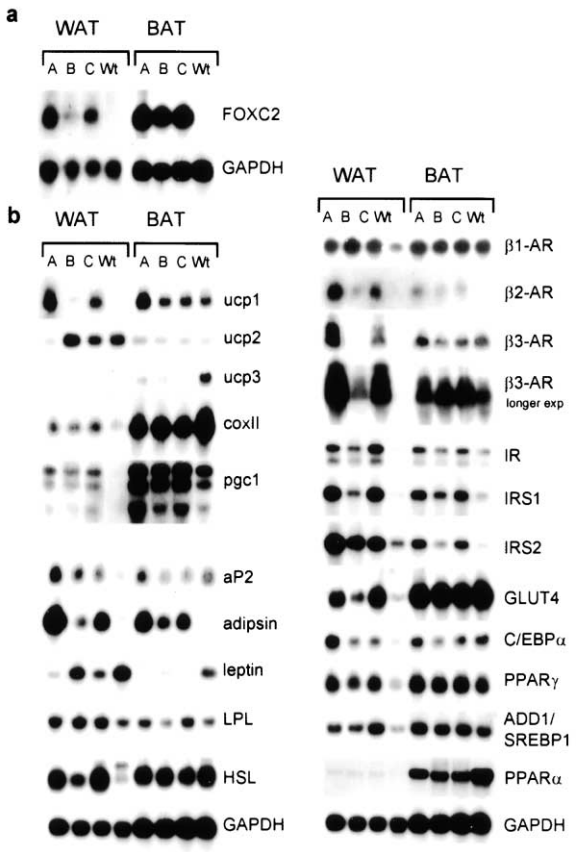

Figure 4. Northern Blot Analysis of mRNA Derived from WAT and BAT of wt and *FOXC2* tg Mice (Founder Lines A, B, and C)

(a) Expression levels of the *FOXC2* transgene in WAT and BAT of wt and tg mice. Note that the human *FOXC2* probe is speific for the mRNA encoded by the human gene and does not cross-react with the murine counterpart *Foxc2*. Twelve micrograms of total RNA/lane, *GAPDH* as an internal control. (b) Relative steady-state mRNA levels in WAT and BAT of wt and tg mice (founder lines A, B, and C). For each probe, the exposure time is the same for WAT and BAT blots, with the exception for the *ucp1* blot. Here, the WAT blot is exposed 40 times longer than the BAT blot. Full names of probes used are found in the corresponding text section. Twelve micrograms of total RNA/lane, *GAPDH* as an internal control.

as compared with wt at 0, 5, 20, 50, and 75 min ($p < 0.001$; Figure 3k). Insulin levels are dramatically lowered in tg mice at all time points ($p < 0.001$; Figure 3l). It is quite extraordinary that tg mice on a high fat diet retain a plasma insulin profile almost identical to that observed when on a standard diet, while wt mice display almost a 3-fold increase in insulin plasma levels (Figures 3j and 3l). Wt mice exhibit a clear increase in glucose levels, while tg mice show a much more modest increase in glucose values (Figures 3i and 3k). These findings highlight *FOXC2*, not only as a gene of importance for adipose tissue distribution, morphology, and gene expression profile, but also, more importantly, as a major regulator of general lipid and glucose metabolism, including protection against diet-induced insulin resistance. They also support the lipotoxicity hypothesis, in that leanness and low levels of FFA are present in the mice (tg) that display the most insulin sensitive phenotype.

More Mitochondria and Higher Oxygen Consumption in WAT from FOXC2 tg Mice

It appears that WAT with an increased expression of *FOXC2* is less efficient in storing triglycerides as compared with wt WAT (Figures 2, 3a, and 3b). This could be due to an elevated metabolism that would dissipate energy through induction of *ucp1* rather than storing it as triglycerides. The induction of *PGC-1*, *PPARγ*, and *coxII* (Figure 4b), genes known to be associated with a stimulated mitochondrial function and biogenesis, urged us to exploit this possibility. Scanning electron microscopy shows a clear reduction in size of adipocytes from tg-A as compared with wild-type adipocytes (43%, $p < 0.001$; Figures 5a, 5b, and 5e). This is in agreement with the tissue sections in Figures 2i and 2j. Transmission electron microscopy reveals an increased amount and size of mitochondria in adipocytes of tg origin (Figures 5c and 5d). The morphology suggests that transgenic WAT could indeed function as a dissipater of excess energy. We measured oxygen consumption in isolated pieces of adipose tissue from tg-A and wt mice; there is almost a 4-fold increase ($p < 0.001$) in oxygen consumption in tg WAT (Figure 5f). There is no significant difference in oxygen consumption in BAT.

To study the regulation of *Foxc2* in wt mice, we set up a real-time quantitative PCR assay. As can be deduced from Figure 5g, steady-state levels of *Foxc2* mRNA in WAT of wt mice on a standard diet (S+/+) is set to 100% and a decrease of 55% ($p = 0.066$) is noted in S+/− mice. An increase of 118% ($p<0.05$) is seen in wt mice on a high fat diet. Since −/− mice have a lethal phenotype, we compared interscapular BAT cell mass between wt and +/− mice and found a significant reduction of BAT cell mass in +/− mice ($p < 0.02$; Figure 5h). This finding demonstrates a gene dose effect on BAT cell mass with regard to *Foxc2*, which strengthens the correlation between *Foxc2* expression and fat cell mass (Figures 3a and 3b). Wt mice on a high fat diet significantly induce their steady-state levels of *Foxc2* mRNA in WAT (Figure 5g). This finding is important since it supports the idea that *Foxc2* can act as a metabolic regulator by sensing the energy content of the diet and, in response to this, alter metabolic efficiency (Figures 3o and 7b).

Increased Sensitivity of the β-Adrenergic/cAMP/Protein Kinase A Pathway

Induction of the cAMP-regulated *ucp1* in WAT, the hypertrophy of BAT, the decrease of intraabdominal WAT depots, and the upregulation of mRNAs encoding β-ARs suggest that an increased sensitivity in the β-adrenergic/cAMP/protein kinase A (PKA) signaling pathway may contribute to the phenotype of *FOXC2* tg mice. In cotransfection experiments, using 3T3-L1 adipocytes, we show that *FOXC2* increases reporter gene activity of a construct driven by the promoter of the *RIα* gene (encodes the regulatory subunit Iα of PKA; Figure 6a), whereas no such regulation could be observed for the *RIIβ* promoter (not shown). We also demonstrate increased *RIα* mRNA levels in adipose tissue from tg mice (Figure 6a, insert) in a dose dependent manner with regard to transgene expression (Figure 4a). This is accompanied by elevated levels of RIα protein in WAT and BAT (Figure 6b). Basal

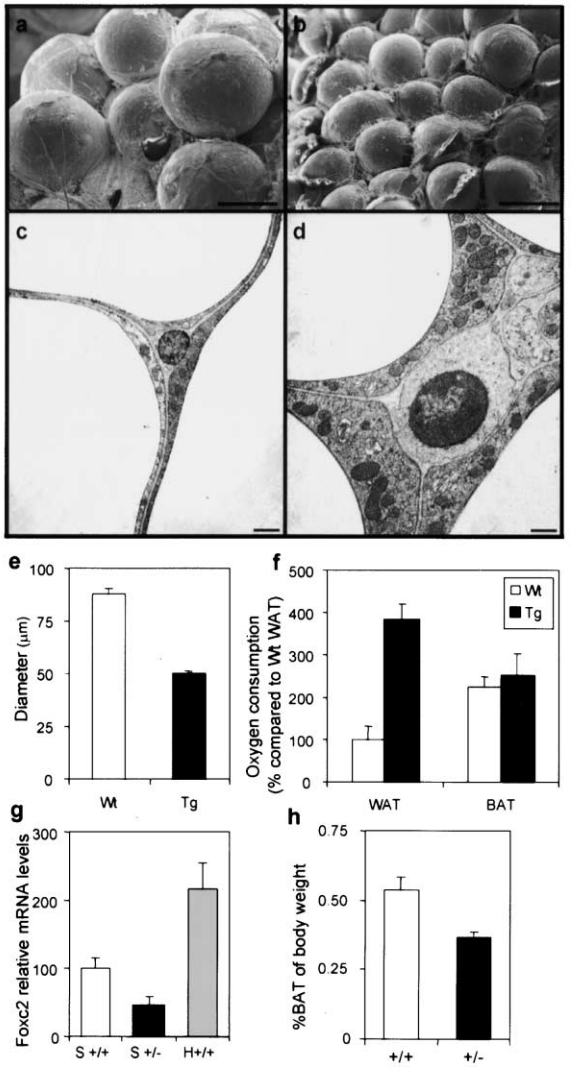

Figure 5. Electron Microscopy and Oxygen Consumption, on 4-Month-Old *FOXC2* tg-A Mice (b and d) and wt Littermates (a and c) as Controls

(a and b) Scanning electron microscopy of intraabdominal WAT from wt and tg mice, respectively. (c and d) Transmission electron microscopy of intraabdominal WAT. The apparent difference in size of the nuclei is due to the relative level of the sections used. The finding of more and larger mitochondria in tg WAT is not influenced by the level of the section used. Scale bars in (a) and (b) equal 50 μm and scale bars in (c) and (d) equal 1 μm. The diameters of adipocytes were measured (e) on images generated by electron microscopy (n = 10). Values are means ± SEM. (f) Oxygen consumption of isolated tissue pieces of white and brown adipose tissue were measured (see "Experimental Procedures"). Values are means ± SEM, n = 4 in each group, and reflect the same number of adipocytes. They were counted after collagenase treatment (see "Experimental Procedures"). In (g), the relative level of *Foxc2* mRNA in wt (+/+) and heterozygous (+/−) mice on a standard diet (S) as well as +/+ mice on a high fat diet (H) was measured using a real time quantitative PCR assay (see "Experimental Procedures"). These mice had been on a high fat diet for approximately 12 weeks. Values are means ± SEM, n = 4 in each group. (h) Weight of interscapular BAT as % of total body weight in mice six weeks of age; wt (+/+) and Foxc2 +/− littermates. Values are means ± SEM, n = 4 in each group.

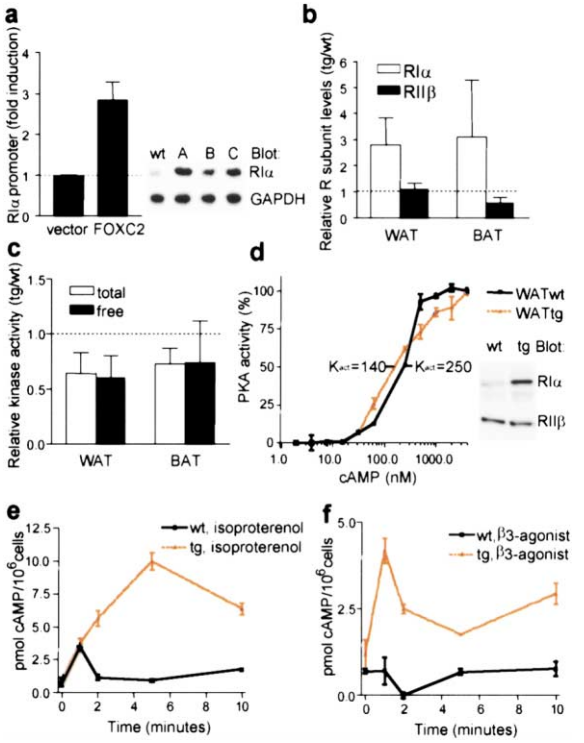

Figure 6. Altered β-Adrenergic Sensitivity, PKA Isozyme Composition, and Activation Kinetics in Adipose Tissue from *FOXC2* tg-A Mice

(a) Left: CAT reporter activity directed from the RIα promoter transfected together with *FOXC2* expression vector or control vector into 3T3-L1 preadipocytes. Data (n = 3 experiments) are CAT values normalized for transfection efficiency, expressed as fold induction. Right: RIα and GAPDH mRNA levels in WAT from wt and the three founder lines (A, B, and C) overexpressing *FOXC2*. (b) Levels of RIα and RIIβ immunoreactive protein in WAT and BAT from tg animals (n = 4) compared to wt littermates (expressed relative to wt levels). (c) Kinase activities using Kemptide as substrate in the presence (total, open bars) or absence (free, solid bars) of 5 μM cAMP. Activities in tg WAT and BAT (n = 4) are shown relative to those in wt littermates. (d) Kinase activities toward Kemptide measured in WAT homogenates from tg and wt littermate mice incubated with increasing concentrations of cAMP. Total cAMP-inducible activity was set to 100%. Right panel, immunoblot demonstrating WAT levels of RIα and RIIβ. Intracellular cAMP levels in adipocyte suspensions prepared from WAT of tg animals and wt littermates (each pooled from 3 animals) and stimulated with either (e) a nonselective β-agonist (isoproterenol, 1 μM) or (f) a β_3-selective agonist (CGP-12177A,1 μM). Equal amounts of cells were withdrawn at different time points (0 to 10 min), in duplicates, mixed with stop buffer, and flash-frozen. Values are means ± SEM.

and total PKA activity is decreased in tg WAT and BAT (Figure 6c). This may be due to an increased sensitivity to activation by cAMP, dissociation, and thereby degradation of PKA holoenzyme (Tasken et al., 1993). The PKA type I holoenzyme ($RI\alpha_2C_2$) binds cAMP with higher affinity and activates more easily than the PKA type II enzyme ($RII\beta_2C_2$) (Dostmann et al., 1990), normally expressed in WAT and BAT (Cummings et al., 1996; Dostmann et al., 1990). Indeed, PKA from WAT of *FOXC2* tg mice with elevated protein levels of RIα (Figure 6d, insert) activates more easily than PKA from WAT of non-tg littermates. A typical experiment is shown (Figure 6d),

with K_{act} of 140 and 250 nM, respectively. The protein levels of RIIβ appear unchanged (Figure 6d, insert). In another experiment, we showed that K_{act} for tg ($n = 4$) and wt ($n = 3$) WAT is 116 ± 9 and 233 ± 9 (±SEM; $p < 0.05$), respectively. Thus, adipocytes from *FOXC2* tg mice will have a lower threshold for PKA activation by adrenergic stimuli as compared with wt littermates due to a PKA isozyme switch. This is in accordance with what has been reported for mice with targeted disruption of the *RII*β gene (Cummings et al., 1996). Stimulation of wt adipocytes with a nonselective β-agonist leads to 4- to 5-fold increase in cAMP levels at 1 min and a rapid termination of the signal. Stimulation of tg adipocytes leads to a strong (10-fold), prolonged, and sustained increase in cAMP levels, which are not terminated at 10 min (Figure 6e). β_3-agonist stimulation of adipocytes prepared from tg WAT displays a distinct increase (4-fold) in cAMP levels with elevated levels over 10 min (Figure 6f). In contrast, little or no β_3-agonist response is observed in adipocytes from wt WAT. These observations are in agreement with the strong upregulation of $\beta_{1\text{-}2}$-AR and the induction of β_3-AR (which is virtually absent in wt) in tg WAT (Figure 4b) and indicate that the sensitivity of β-adrenergic/cAMP/PKA pathway in WAT from *FOXC2* tg mice is increased at several levels.

Discussion

From the data presented here, it is clear that *FOXC2* regulates, directly or indirectly, several aspects of adipocyte metabolism. Even though it is likely that other pathways/genes are involved, the induction of *ucp1* in WAT, the hypertrophy of BAT, the decrease of intraabdominal WAT depots, the upregulation of mRNAs encoding β-adrenergic receptors, and the increased oxygen consumption in tg WAT suggest that an increased sensitivity in a β-adrenergic/cAMP/protein kinase A (PKA) pathway, at least in part, can explain the phenotype of mice overexpressing *FOXC2*. The finding of an isoenzyme shift that will lower the threshold for PKA activation by adrenergic stimuli and the increased sensitivity for β-adrenergic agonists, in adipocytes from tg mice, provides further support for this hypothesis (Figures 6a–6d). Indeed, animals subjected to chronic adrenergic stimulation show increased BAT depots and decreased WAT stores with multilocular BAT-like cells (Himms-Hagen et al., 1994). The effects of chronic adrenergic stimulation can in part be derived from an increased BAT cell proliferation, *ucp1* induction, and stimulation of lipolysis. This will lead to loss of body fat, increased glucose tolerance, and decreased serum triglycerides, through a process that mimics BAT adaptive thermogenesis (Lowell and Flier, 1997; Yoshida et al., 1994). While the phenotype in animals under chronic adrenergic stimulation, can, in large part, be attributed to an increased energy turnover mediated through cell surface located β-ARs, the metabolic changes seen in *FOXC2* tg mice are due to an increased expression level of an intracellular transcription factor that exerts a pleiotropic effect on gene expression in BAT and WAT. The sensitivity of the β-adrenergic-cAMP-protein kinase A (PKA) pathway is enhanced, in adipocytes, on several levels, as indicated by the increased sensitivity for both a nonselective β-agonist as well as for a selctive β_3-agonist (Figures 6e and 6f) as well as altered PKA holoenzyme composition (Figures 6a–6d). An alternative explanation to our findings would be a *PGC1*-induced increase of *PPAR*γ which, together, would activate *ucp1* (Figure 4b) (Puigserver et al., 1998). An increased intracellular level of FFA, as suggested by the observed induction of *HSL* (Figure 4b), would provide *PPAR*γ with endogenous ligand. This explanation gains support from the finding that ectopic expression of *PGC1* in white adipose cells, in vitro, activates expression of *ucp1* (Puigserver et al., 1998). As opposed to our in vivo findings, these authors demonstrate a reduction in steady-state levels of *aP2* mRNA. Nevertheless, it is possible that an increased adrenergic sensitivity, on several levels, in conjunction with *PGC1*, *PPAR*γ, and *PPAR*α activation (Figure 4b) contributes to induce a WAT phenotype that will lead to dissipation of energy through an increased β-oxidation and uncoupling. This is supported by the observations that adipocytes of transgenic origin contain more and larger mitochondria (Figures 5c and 5d) and that the oxygen consumption is significantly elevated in such adipocytes (Figure 5f).

We speculate that increased mRNA levels for *IR*, *IRS1*, *IRS2*, and *GLUT4* (Figure 4b) would lead to enlarged WAT depots with increased insulin sensitivity, as seen in the aP2-GLUT4 mice (Shepherd et al., 1993). In *FOXC2* tg mice, the imminent threat of obesity and insulin resistance, due to activation of genes that stimulate adipocyte differentiation (*C/EBP*α, *PPAR*γ, and *ADD1/SREBP1*) and lipid accumulation (*aP2* and *adipsin*), is counteracted by factors that enhance energy dissipation (*ucp1* and *pgc1*). Thus, the *FOXC2* tg mice would have been obese and insulin sensitive had it not been for the increased BAT and induction of *ucp1* in WAT, which will supply means by which energy can be dissipated. The mRNA levels for *ucp1*, $\beta_{2\text{-}3}$-*AR*, *C/EBP*α, *RI*α, *adipsin*, *IRS1*, and *GLUT4* all demonstrate a dose-response relation with regard to expression of the transgene (Figures 4b and 6a), which could reflect a direct regulation by *FOXC2* (Figure 7a), whereas indirect effects could be involved in regulation of the other genes (Figure 4b). It is possible that *FOXC2* directly, through transcriptional activation of "master" genes, controls a network that regulates energy turnover (*ucp1*, $\beta_{2\text{-}3}$-*AR*, and *RI*α), differentiation (*C/EBP*α), metabolism (*adipsin*), and insulin sensitivity (*IRS1* and *GLUT4*) in adipocytes (Figure 7a). It is interesting to note the almost complete concordance between the insulin and glucose profiles for tg mice, regardless of diet (Figures 3i–3l), whereas wt mice develop a pronounced insulin resistance when fed a high fat diet (Figures 3k and 3l). Thus, it is possible that factors that enhance energy dissipation can sense the metabolic status of the animal. The upregulation of *Foxc2* mRNA levels in animals on a high fat diet supports this view (Figure 5g)

Thrifty genes are thought to conserve energy during periods of famine whereas they constitute a risk for developing obesity related conditions, e.g., type 2 diabetes, when energy is abundant. It has been speculated that there exists a balance between factors that conserve—"thrifty" genes—and factors that mobilize energy—"anti-thrifty"—genes. This balance allows survival during periods of food deprivation, frequently encountered during evolution, without the maladaptive

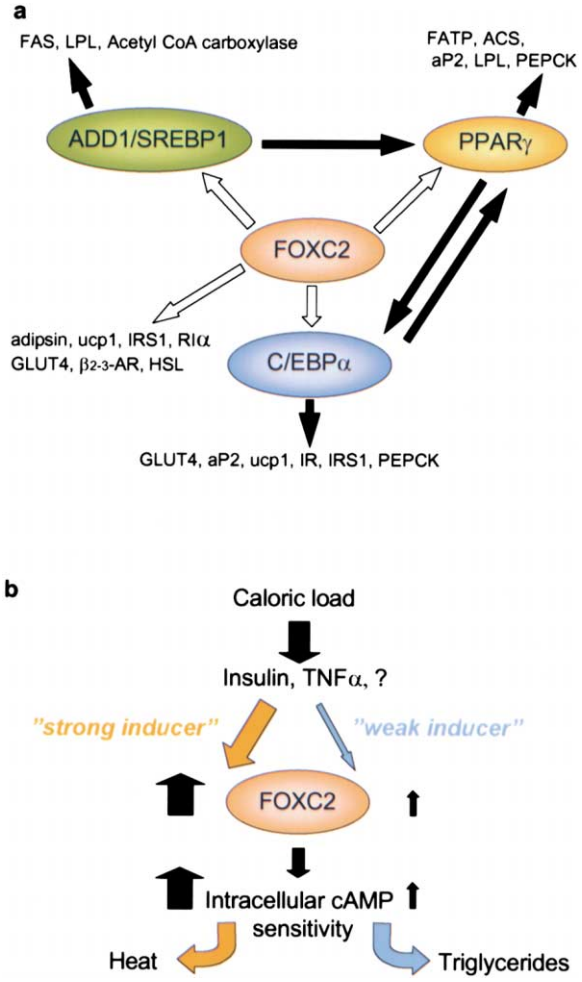

Figure 7. Hypothetical Action of *FOXC2* in an Adipocyte Gene Regulatory Network

(a) Filled arrows indicate known positive transcriptional regulation. Open arrows represent a proposed action of *FOXC2*. *ADD1/SREBP1* both activate transcription of acetyl CoA carboxylase (Lopez et al., 1996), fatty acid synthase (*FAS*), and lipoprotein lipase (*LPL*) genes, and increases the transcriptional activity of *PPARγ* (Fajas et al., 1999). PPARγ activates transcription of fatty acid transport protein (FATP), acyl-CoA synthetase genes (Martin et al., 1997) (*ACS*), adipocyte fatty acid binding protein 422/aP2 (Tontonoz et al., 1994) (*aP2*), *LPL* (Schoonjans et al., 1996), and phosphoenolpyruvate carboxykinase (Tontonoz et al., 1995) (*PEPCK*). C/EBPα activates insulin-responsive glucose transporter-4 (Kaestner et al., 1990) (*GLUT4*), *aP2*(Christy et al., 1989), uncoupling protein-1 (Yubero et al., 1994) (*UCP1*), the insulin receptor (*IR*), insulin receptor substrate-1 (Wu et al., 1999b) (*IRS1*), and *PEPCK* (Park et al., 1990). A positive feedback loop between *C/EBPα* and *PPARγ* has been suggested (Wu et al., 1999b). (b) We propose that a strong induction of *FOXC2* in response to a caloric load leads to a metabolic situation in which a large portion of the ingested calories would be dissipated as heat whereas a weaker induction induces conservation of the caloric load as triglycerides.

consequences of an excess of adipose tissue in times when food is available (Flier, 1995; Friedman and Halaas, 1998; Zimmet and Alberti, 1997). Since the total body lipid content in *FOXC2* tg mice, on a standard diet, is reduced from 30% to 10% (Figure 3c), without any significant change in body weight or food consumption, there must exist a net increase in energy expenditure. Furthermore, tg mice appear to be able to regulate energy efficiency when fed a high fat diet, as demonstrated by the reduced weight gain to food consumed ratio (Figure 3o). In this sense, *FOXC2* could be regarded as an "anti-thrifty" gene. This is further supported by the findings that *FOXC2* tg mice demonstrate a relative resistance to diet-induced weight gain (Figure 3m) as well as diet-induced insulin resistance (Figures 3k and 3l). One possible mechanism by which this could be achieved is through the *FOXC2*-induced upregulation of mRNA levels for *HSL* in WAT (Figure 4b), which could provide means for an increased flow of FFA to the mitochondria, where *ucp1* would dissipate its energy content. An increase in number and/or biological activity of mitochondria, as reflected by increased levels of *coxII* and *pgc1* (Figure 4b), would further enhance this process. The relevance of this hypothesis is underscored by the fact that tg WAT contains more and larger mitochondria (Figures 5c and 5d) and has an increased oxygen consumption (Figure 5f).

Why is it that *FOXC2* tg mice do not increase their food intake to a level that would compensate for the loss of adipose tissue? One explanation could be that increased *FOXC2* expression affects satiety signaling to CNS. It has been speculated that BAT produces an appetite suppressing signal since BAT-ablated mice are hyperphagic (Flier, 1995). This would mean that although *FOXC2* tg mice do not eat more than their wild-type littermates, they eat less than they would need to for preservation of an energy store, comparable in size to that of their wt littermates. This could be explained by increased expression of a hypothetical appetite suppressing signal from the enlarged BAT depot.

Based on the data reported here, *FOXC2* should be regarded as a candidate gene for obesity, insulin resistance, and type 2 diabetes. The phenotype induced by increasing *FOXC2* expression in adipose tissue supports the hypothesis of lipotoxicity, since a decrease in total body lipid content and levels of FFA leads to increased insulin sensitivity (Figures 3i–3l; Unger and Orci, 2000; Boden, 1997). In this context, it is interesting to note that altering expression of a single gene in adipose tissue results in systemic changes of glucose, insulin, and lipid metabolism in a way that protects against the consequences of caloric overload. We propose a model in which the degree of *FOXC2* induction, in response to a caloric load, determines the efficiency by which these calories are converted to triglycerides (Figure 7b). In this way, a pronounced *FOXC2* induction will act as a defense against an increasing adipose tissue mass. The degree of adrenergic sensitivity, regulated by FOXC2, could be regarded as a cellular "set point" for metabolism in adipocytes. *FOXC2* also constitutes novel drug target. Data presented here demonstrate that *FOXC2* is likely to play a role as a metabolic regulator and possibly a factor that can induce adaptive thermogenesis—with a potential capacity of counteracting not only obesity, insulin resistance, hypertriglyceridemia, increased plasma levels of FFA, and diet-induced insulin resistance, but also type 2 diabetes.

Experimental Procedures

Cloning and DNA Construct

A human adipose tissue λgt11 cDNA library (Clontech) was screened with a probe mixture corresponding to the conserved forkhead do-

main derived from *FOXC1*, *FOXD1*, *FOXL1*, and *FOXA1*. Hybridization was carried out at low stringency, i.e., 6 × SSC at 60°C, posthybridization washes at 0.5 × SSC at 60°C. One of the positive recombinants harboring a 2.1 kb insert was subcloned and sequenced. A 5.4 kb EcoRV-SmaI fragment was excised from pBluescript II SK(+) vector containing the 5.4 kb promoter/enhancer of the mouse *aP2* gene and ligated into the EcoRV-SpeI blunt site of pBluescript II SK(+) vector containing the 2.1 kb *FOXC2* cDNA. A 7.6 kb XhoI blunt fragment containing the aP2 promoter/enhancer followed by the *FOXC2* cDNA was excised from the above plasmid and ligated into the EcoRV site of the pCB6+ vector, which contains a polyadenylation signal from the human growth hormone gene. After these procedures, the resulting 8.2 kb fragment, harboring the *aP2-FOXC2* construct with polyadenylation signal, was flanked by the unique sites NotI and AgeI. The plasmid was sequenced over ligation sites.

Transgenic Mice

Construct DNA (aP2-FOXC2), purified using Qiagen kit, according to manufacturer's instructions, was injected into the male pronucleus of (C57BL/6J x CBA) F_1 zygotes, cultured overnight and transferred to pseudopregnant females. Tg founder lines were backcrossed to C57BL/6J for four generations. Mice were feed a standard chow with 4% (w/w) fat content. In experiments with high fat diet, mice were fed a chow with 35.9% (w/w) fat (Research Diets) for 9 weeks. In the glucose tolerance experiment (Figure 3), mice were on their respective diets for 14 weeks. High fat chow has a total energy content of 23.4 kJ/g, standard diet 12.6 kJ/g.

Histology

Tissues were fixed overnight in 4% paraformaldehyde in PBS at 4°C, dehydrated, embedded in paraffin, sectioned (6–8 μm), and stained with haematoxylin and eosin.

Serum and Lipid Analysis

Plasma insulin was determined radioimmunochemically with the use of a guinea pig anti-rat insulin antibody, ^{125}I-labeled porcine insulin as tracer and rat insulin as standard (Linco). Free and bound radioactivity was separated by use of an anti-IgG (goat anti-guinea pig) antibody (Linco). The sensitivity of the assay is 17 pmol/l and the coefficiency of variation is less than 3% at both low and high levels. Plasma glucose was determined with the glucose oxidase method, and FFAs were measured photometrically. Plasma glucagon was determined radioimmunochemically with the use of a guinea pig antiglucagon antibody specific for pancreatic glucagon, ^{125}I-labeled-glucagon as tracer, and glucagon standard (Linco). Free and bound radioactivity was separated by use of an anti-IgG (goat anti-guinea pig) antibody (Linco). The sensitivity of the assay is 7.5 pg/ml and the coefficient of variation is less than 9%. Blood levels of serum cholesterol and triglycerides were determined by standard, fully enzymatic techniques. Total body lipid was assessed using alcoholic hydroxide digestion with saponification of all lipids and neutralization, followed by enzymatic determination of glycerol.

Intravenous Glucose Tolerance Test

The mice were anesthetized with an intraperitoneal injection of midazolam (0.4 mg/mouse) (Hoffman-La-Roche) and a combination of fluanison (0.9 mg/mouse) and fentanyl (0.02 mg/mouse) (Janssen). Thereafter, a blood sample was taken from the retrobulbar, intraorbital, capillary plexus in heparinized tubes, whereafter D-glucose 1g/kg (British Drug Houses) was injected rapidly intravenously. New blood samples were taken after 1, 5, 20, 50, and 75 min. Following immediate centrifugation at 4°C, plasma was separated and stored at −20°C or until analysis.

Northern Blot

cDNA probes for mouse *Foxc2*, *aP2*, *ADD-1/SREBP1*, *coxII*, *adipsin*, $\beta_{1\text{-}3}$*-AR*, *GLUT4*, *IR*, *IRS1*, *IRS2*, and *PPARα* were prepared by RT-PCR by use of first-strand cDNA from mouse epididymal fat poly(A)$^+$ RNA. The PCR primers used to generate these probes were as follows. *Foxc2*: 5′ primer, GCTTCGCCTCCTCCATGGGAA and 3′ primer, GGTTACAAATCCGCACTCGTT (GenBank # Y08222). *aP2*: 5′ primer, CTCCTGTGCTGCAGCCTTTCTC and 3′ primer, CGTAACTCACCACCACCAGCTTGTC (GenBank # M13261). *ADD1/SREBP1*: 5′ primer, GCCAACTCTCCTGAGAGCTT and 3′ primer, CTCCTGCTTGAGCTTCTGGTT (GenBank # AB017337). *CoxII*: 5′ primer, CCATTCCAACTTGGTCTACAA and 3′ primer, GGAACCATTTCTAGGACAATG (GenBank # J01420). *Adipsin*: 5′ primer, CGAGGCCGGATTCTGGGTGGCCAG and 3′ primer, TCGATCCACATCCGGTAGGATG (GenBank # X04673). β_1*-AR*: 5′ primer, CGGCTGCAGACGCTCACCAA and 3′ primer, CGCCACCAGTGCATGAGGAT (GenBank # L10084). β_2*-AR*: 5′ primer, GCTGCAGAAGATAGACAAAT and 3′ primer, GGGATCCTCACACAGCAGTT (GenBank # X15643). β_3*-AR*: 5′ primer, CTGCTAGCATCGAGACCTT and 3′ primer, CGAGCATAGACGAAGAGCAT (GenBank # X60438). *GLUT4*: 5′ primer,CTCAGCAGCGAGTGACTGGGAC and 3′ primer, CCCTGAGTAGGCGCCAATGAGG (GenBank # D28561). *IR*: 5′ primer, GTAGCCTGATCATCAACATCCG and 3′ primer, CCTGCCCATCAAACTCTGTCAC (GenBank # J05149). *IRS1*: 5′ primer, ATGGCGAGCCCTCCGGATACCG and 3′ primer, CCTCTCCAACGCCAGAAGCTGCC (GenBank # X69722). *IRS2*: 5′ primer, GGATAATGGTGACTATACCGAGA and 3′ primer, CTCACATCGATGGCGATATAGTT (GenBank # AF090738). *PPARα*: 5′ primer, TCCCTTGTAGCCTTTTGTCAT and 3′ primer, AAGCCATTGCCGTACGCGAT (GenBank # X75293). All other probes used have been provided by researchers mentioned under "Acknowledgments." cDNA probes were radiolabeled with [α-^{32}P]dCTP (3000 Ci/mmol) by the random labeling method. Total RNA from mice in each group was pooled, and aliquots of 12 μg were separated on an agarose gel. The filters were hybridized with ^{32}P-labeled probe (10^6 cpm/ml) for 1 hr at 62°C with QuikHyb solution (Stratagene) and washed with 0.1% SDS/0.1 × SSC at 62°C for 3 × 20 min. Adipocytes and stroma/vascular cells used in Figure 1c were isolated by collagenase digestion (1mg/ml, Sigma C6885) in Dulbecco's modified Eagle's medium at 37°C for 60 min, followed by centrifugation (1500 rpm 10 min), rendering the adipocytes floating at the top and the stroma/vascular fraction in the pellet. For analysis of *Foxc2* mRNA regulation (Figure 1d), 3T3-L1 cells were grown to confluence and differentiated using a combination of dexametasone, insulin and, metyl-isobutylxanthine for three days, followed by insulin alone for three days. Since the combination of agents used to induce differentiation also increased *Foxc2* mRNA (not shown), cells were continued for four days without any stimulus to fully mature adipocytes at day ten using standard protocols. At day eleven (five days after removal of the differentiation mixture), cells were treated with various agents, subjected to Northern blotting and analysis of the *Foxc2* signal by β-scintillation counting in a dot-matrix β-plate counter (Instant Imager, Packard).

Real-Time Quantitative RT-PCR

Reverse transcription of 1 μg total RNA was carried out using a 1st Strand cDNA Synthesis Kit for RT-PCR (AMV) (Roche, #1483188). 0.25 μl and 7.8 nl of the first strand cDNA synthesis were used respectively per 50 μl of PCR reaction (TaqMan Universal PCR Master Mix, Applied Biosystems) to determine *Foxc2* and 18S ribosomal RNA levels using the ABI Prism 7700 sequence detection system. The primer sequences used for *Foxc2* detection were as follows. Forward: 5′-GAAAGCGCCCCTCTCTCAG-3′ and reverse: 5′-TGCGGATAAGTTACCTGCGA-3′; for 18S ribosome, forward: 5′-AGTCCCTGCCCTTTGTACACA-3′ and reverse: 5′-GATCCGAGGGCCTCACTAAAC-3′. The probe sequences for *Foxc2* and 18S ribosome were 5′-6FAM-ACCAGGAGCAGAGAGCTCCGTGCAA-TAMRA-3′ and 5′-6FAM-CGCCCGTCGCTACTACCGATTGG-TAMRA-3′, respectively.

Transfections and Reporter Gene Analysis

Nonconfluent cultures of 3T3-L1 adipocytes were transfected with a CAT reporter (pCAT) driven by the human *RIα* proximal promoters upstream of the alternatively spliced 1a and 1b leader exons (nucleotides 1509 to 2470 GenBank # Y07641). To control transfection efficiency, a pGL3 control (Promega) luciferase-encoding vector was used. In cotransfections, a *FOXC2* expression vector or vector void of insert was used. Transfections were carried out using lipofectamine (Gibco), followed by CAT and luciferase assays.

Electron Microscopy

Tissue pieces for scanning electron microscopy were prepared with the OTOTO method, i.e., repeated cycles with 1% OsO_4 in 0.1 M cacodylate and a saturated solution of thiocarbhydrazide in water.

The samples were dehydrated in ethanol and infiltrated with hexamethyldisilazane. The dried samples were mounted with carbon adhesive tape on aluminum stubs and examined in a Zeiss 982 Gemini field emission scanning electron microscope without previous sputter coating. Tissue pieces for transmission electron microscopy were fixed with an aldehyde mixture of 2.5% glutaraldehyde and 2% paraformaldehyde, with the addition of 0.02% sodium azide, in 0.05 M Na cacodylate (pH 7.2), for 24 hr. Post-fixation of specimens intended for plastic embedding was obtained with a 1 + 1 mixture of 1% OsO_4 and 1% potassium ferrocyanide in 0.1 M Na cacodylate for 3 hr, followed by en bloc staining with 1% uranyl acetate in water for 2 hr. After ethanol dehydration, the specimens were infiltrated with Agar 100 epoxy resin (Agar Aids) and cured by heat. Ultrathin sections were obtained with a Reichert ultramicrotome fitted with a diamond knife and were contrasted with uranyl acetate and lead citrate before examination in a Zeiss CEM 902 electron microscope.

Oxygen Consumption

Transgenic mice and littermates (4 months old) were sacrificed and adipose tissue pieces ($\sim$1 mg each) were prepared under sterile conditions, washed, and incubated in Parker Medium 199 (SBL, Stockholm), supplemented with 12.5 mmol/L $NaHCO_3$, 10 mmol/L HEPES (Sigma), 1% human serum albumin (Immuno AG, Vienna), 0.1 mg/ml cephalotin (Sigma), and 7175 pmol/l insulin (Actrapid, Novo Nordisk, Bagsvaerd, Denmark), at 37°C for at least two hours before measurement. O_2 consumption for approximately ten pieces at a time was recorded polarographically by an electrode (Radiometer E5046) in a thermostated 0.4 ml glass vessel filled with incubation medium, stirred by a magnetic stirrer. After this, a collagenase digestion (1 mg/ml, Sigma C6885) in DMEM at 37°C for 60 min was performed to determine the number of adipocytes in each of the tissue pieces.

PKA and cAMP Levels

WAT and BAT were treated by a Polytron tissue homogenizer (3 $\times$ 15 s) and sonicated, on ice, in a buffer containing 10 mM potassium phopsphate (pH 6.8), 150 mM sodium chloride, 1 mM EDTA, 10 mM CHAPS, and protease inhibitors, and centrifuged (15,000 $\times$ g) to remove unsoluble material. Protein concentrations were determined by Bradford assays (BioRad). For immunoblotting, 30 μg of protein was separated by 10% SDS-PAGE, transferred to PVDF membranes, and incubated with anti-RIα and anti-RIIβ mAb. Primary antibodies were detected by HRP-conjugated anti-mouse IgG (Transduction Laboratories, 1:5000) and ECL (Amersham). PKA activity was measured using Kemptide (Leu-Arg-Arg-Ala-Ser-Leu-Gly) as substrate in the absence or presence of varying concentrations of cAMP. The low levels of activity not inhibited by PKI (2 μM) were subtracted to determine PKA-specific activity. Intracellular cAMP levels were determined by radioimmunoassay (Cyclic AMP Flashplate, SMP 004, New England Nuclear, Zaventem, Belgium) according to the manufacturer's instructions and measured after stimulation with a nonselective β-agonist (isoproterenol, 1 μM) or a selective β_3-agonist (CGP-12177A, 1 μM). Equal amounts of cells were withdrawn at different time points, mixed with stop buffer, and flash-frozen.

Statistical Analysis

A two-tailed Student's t test was used to calculate p values.

Acknowledgments

We thank B. Cannon, L. Groop, and L.P. Kozak for valuable discussion; M. Axelsson for help with measuring oxygen consumption; J. Borén for analyzing serum samples; B.R. Johansson for expert assistance with electron microscopy; N. Miura for kindly providing Foxc2 +/− mice; L. Kvist, L. Bengtsson, and U. Gustavsson for expert technical assistance; and J. Gimble, D. Grujie, C. Holm, L.P. Kozak, N.-G. Larsson, J. Schwartz, and B.M. Spiegelman for sharing probes with us. This work was made possible with support from The Swedish Medical Research Foundation, The Arne and IngaBritt Lundberg Foundation, The Juvenile Diabetes Foundation, The Wallenberg Foundation, Pharmacia & Upjohn, Inc., and a Junior Individual Grant from The Swedish Foundation for Strategic Research to S.E.

Received March 1, 2001; revised August 2, 2001.

References

Abbott, W.G., and Foley, J.E. (1987). Comparison of body composition, adipocyte size, and glucose and insulin concentrations in Pima Indian and Caucasian children. Metabolism *36*, 576–579.

Boden, G. (1997). Role of fatty acids in the pathogenesis of insulin resistance and NIDDM. Diabetes *46*, 3–10.

Bouchard, C., Tremblay, A., Despres, J.P., Nadeau, A., Lupien, P.J., Theriault, G., Dussault, J., Moorjani, S., Pinault, S., and Fournier, G. (1990). The response to long-term overfeeding in identical twins. N. Engl. J. Med. *322*, 1477–1482.

Christy, R.J., Yang, V.W., Ntambi, J.M., Geiman, D.E., Landschulz, W.H., Friedman, A.D., Nakabeppu, Y., Kelly, T.J., and Lane, M.D. (1989). Differentiation-induced gene expression in 3T3–L1 preadipocytes: CCAAT/enhancer binding protein interacts with and activates the promoters of two adipocyte-specific genes. Genes Dev. *3*, 1323–1335.

Coe, N.R., Simpson, M.A., and Bernlohr, D.A. (1999). Targeted disruption of the adipocyte lipid-binding protein (aP2 protein) gene impairs fat cell lipolysis and increases cellular fatty acid levels. J. Lipid Res. *40*, 967–972.

Cummings, D.E., Brandon, E.P., Planas, J.V., Motamed, K., Idzerda, R.L., and McKnight, G.S. (1996). Genetically lean mice result from targeted disruption of the RII beta subunit of protein kinase A. Nature *382*, 622–626.

Dostmann, W.R., Taylor, S.S., Genieser, H.G., Jastorff, B., Doskeland, S.O., and Ogreid, D. (1990). Probing the cyclic nucleotide binding sites of cAMP-dependent protein kinases I and II with analogs of adenosine 3′,5′-cyclic phosphorothioates. J. Biol. Chem. *265*, 10484–10491.

Enerback, S., Ohlsson, B.G., Samuelsson, L., and Bjursell, G. (1992). Characterization of the human lipoprotein lipase (LPL) promoter: evidence of two cis-regulatory regions, LP-alpha and LP-beta, of importance for the differentiation-linked induction of the LPL gene during adipogenesis. Mol. Cell. Biol. *12*, 4622–4633.

Enerback, S., Jacobsson, A., Simpson, E.M., Guerra, C., Yamashita, H., Harper, M.E., and Kozak, L.P. (1997). Mice lacking mitochondrial uncoupling protein are cold-sensitive but not obese. Nature *387*, 90–94.

Fajas, L., Schoonjans, K., Gelman, L., Kim, J.B., Najib, J., Martin, G., Fruchart, J.C., Briggs, M., Spiegelman, B.M., and Auwerx, J. (1999). Regulation of peroxisome proliferator-activated receptor gamma expression by adipocyte differentiation and determination factor 1/sterol regulatory element binding protein 1: implications for adipocyte differentiation and metabolism. Mol. Cell. Biol. *19*, 5495–5503.

Flier, J.S. (1995). The adipocyte: storage depot or node on the energy information superhighway? Cell *80*, 15–18.

Friedman, J.M., and Halaas, J.L. (1998). Leptin and the regulation of body weight in mammals. Nature *395*, 763–770.

Hamann, A., Flier, J.S., and Lowell, B.B. (1996). Decreased brown fat markedly enhances susceptibility to diet-induced obesity, diabetes, and hyperlipidemia. Endocrinology *137*, 21–29.

Himms-Hagen, J., Cui, J., Danforth, E., Jr., Taatjes, D.J., Lang, S.S., Waters, B.L., and Claus, T.H. (1994). Effect of CL-316,243, a thermogenic beta 3-agonist, on energy balance and brown and white adipose tissues in rats. Am J. Physiol. *266*, R1371–R1382.

Iida, K., Koseki, H., Kakinuma, H., Kato, N., Mizutani-Koseki, Y., Ohuchi, H., Yoshioka, H., Noji, S., Kawamura, K., Kataoka, Y., et al. (1997). Essential roles of the winged helix transcription factor MFH-1 in aortic arch patterning and skeletogenesis. Development *124*, 4627–4638.

Kaestner, K.H., Christy, R.J., and Lane, M.D. (1990). Mouse insulin-responsive glucose transporter gene: characterization of the gene

and trans-activation by the CCAAT/enhancer binding protein. Proc. Natl. Acad. Sci. USA *87*, 251–255.

Kim, J.B., and Spiegelman, B.M. (1996). ADD1/SREBP1 promotes adipocyte differentiation and gene expression linked to fatty acid metabolism. Genes Dev. *10*, 1096–1107.

Levine, J.A., Eberhardt, N.L., and Jensen, M.D. (1999). Role of nonexercise activity thermogenesis in resistance to fat gain in humans. Science *283*, 212–214.

Lin, F.T., and Lane, M.D. (1994). CCAAT/enhancer binding protein alpha is sufficient to initiate the 3T3-L1 adipocyte differentiation program. Proc. Natl. Acad. Sci. USA *91*, 8757–8761.

Lopez, J.M., Bennett, M.K., Sanchez, H.B., Rosenfeld, J.M., and Osborne, T.E. (1996). Sterol regulation of acetyl coenzyme A carboxylase: a mechanism for coordinate control of cellular lipid. Proc. Natl. Acad. Sci. USA *93*, 1049–1053.

Lowell, B.B., and Flier, J.S. (1997). Brown adipose tissue, beta 3-adrenergic receptors, and obesity. Annu. Rev. Med. *48*, 307–316.

Martin, G., Schoonjans, K., Lefebvre, A.M., Staels, B., and Auwerx, J. (1997). Coordinate regulation of the expression of the fatty acid transport protein and acyl-CoA synthetase genes by PPARalpha and PPARgamma activators. J. Biol. Chem. *272*, 28210–28217.

Moitra, J., Mason, M.M., Olive, M., Krylov, D., Gavrilova, O., Marcus-Samuels, B., Feigenbaum, L., Lee, E., Aoyama, T., Eckhaus, M., et al. (1998). Life without white fat: a transgenic mouse. Genes Dev. *12*, 3168–3181.

Murray, I., Sniderman, A.D., Havel, P.J., and Cianflone, K. (1999). Acylation stimulating protein (ASP) deficiency alters postprandial and adipose tissue metabolism in male mice. J. Biol. Chem. *274*, 36219–36225.

O'Rahilly, S. (1997). Diabetes in midlife: planting genetic time bombs. Nat. Med. *3*, 1080–1081.

Osuga, J., Ishibashi, S., Oka, T., Yagyu, H., Tozawa, R., Fujimoto, A., Shionoiri, F., Yahagi, N., Kraemer, F.B., Tsutsumi, O., and Yamada, N. (2000). Targeted disruption of hormone-sensitive lipase results in male sterility and adipocyte hypertrophy, but not in obesity. Proc. Natl. Acad. Sci. USA *97*, 787–792.

Park, E.A., Roesler, W.J., Liu, J., Klemm, D.J., Gurney, A.L., Thatcher, J.D., Shuman, J., Friedman, A., and Hanson, R.W. (1990). The role of the CCAAT/enhancer-binding protein in the transcriptional regulation of the gene for phosphoenolpyruvate carboxykinase (GTP). Mol. Cell. Biol. *10*, 6264–6272.

Puigserver, P., Wu, Z., Park, C.W., Graves, R., Wright, M., and Spiegelman, B.M. (1998). A cold-inducible coactivator of nuclear receptors linked to adaptive thermogenesis. Cell *92*, 829–839.

Ross, S.R., Graves, R.A., Greenstein, A., Platt, K.A., Shyu, H.L., Mellovitz, B., and Spiegelman, B.M. (1990). A fat-specific enhancer is the primary determinant of gene expression for adipocyte P2 in vivo. Proc. Natl. Acad. Sci. USA *87*, 9590–9594.

Schoonjans, K., Peinado-Onsurbe, J., Lefebvre, A.M., Heyman, R.A., Briggs, M., Deeb, S., Staels, B., and Auwerx, J. (1996). PPARalpha and PPARgamma activators direct a distinct tissue-specific transcriptional response via a PPRE in the lipoprotein lipase gene. EMBO J. *15*, 5336–5348.

Shepherd, P.R., Gnudi, L., Tozzo, E., Yang, H., Leach, F., and Kahn, B.B. (1993). Adipose cell hyperplasia and enhanced glucose disposal in transgenic mice overexpressing GLUT4 selectively in adipose tissue. J. Biol. Chem. *268*, 22243–22246.

Shimomura, I., Hammer, R.E., Richardson, J.A., Ikemoto, S., Bashmakov, Y., Goldstein, J.L., and Brown, M.S. (1998). Insulin resistance and diabetes mellitus in transgenic mice expressing nuclear SREBP-1c in adipose tissue: model for congenital generalized lipodystrophy. Genes Dev. *12*, 3182–3194.

Susulic, V.S., Frederich, R.C., Lawitts, J., Tozzo, E., Kahn, B.B., Harper, M.E., Himms-Hagen, J., Flier, J.S., and Lowell, B.B. (1995). Targeted disruption of the beta 3-adrenergic receptor gene. J. Biol. Chem. *270*, 29483–29492.

Tasken, K., Andersson, K.B., Skalhegg, B.S., Tasken, K.A., Hansson, V., Jahnsen, T., and Blomhoff, H.K. (1993). Reciprocal regulation of mRNA and protein for subunits of cAMP-dependent protein kinase (RI alpha and C alpha) by cAMP in a neoplastic B cell line (Reh). J. Biol. Chem. *268*, 23483–23489.

Tontonoz, P., Hu, E., and Spiegelman, B.M. (1994). Stimulation of adipogenesis in fibroblasts by PPAR gamma *2*, a lipid-activated transcription factor. Cell *79*, 1147–1156.

Tontonoz, P., Hu, E., Devine, J., Beale, E.G., and Spiegelman, B.M. (1995). PPAR gamma 2 regulates adipose expression of the phosphoenolpyruvate carboxykinase gene. Mol. Cell. Biol. *15*, 351–357.

Unger, R.H., and Orci, L. (2000). Lipotoxic disease of nonadipose tissues in obesity. Int. J. Obes. Relat. Metab. Disord. *24*, 28–32.

Winnier, G.E., Hargett, L., and Hogan, B.L. (1997). The winged helix transcription factor MFH1 is required for proliferation and patterning of paraxial mesoderm in the mouse embryo. Genes Dev. *11*, 926–940.

Wu, Z., Puigserver, P., Andersson, U., Zhang, C., Adelmant, G., Mootha, V., Troy, A., Cinti, S., Lowell, B., Scarpulla, R.C., and Spiegelman, B.M. (1999a). Mechanisms controlling mitochondrial biogenesis and respiration through the thermogenic coactivator PGC-1. Cell *98*, 115–124.

Wu, Z., Rosen, E.D., Brun, R., Hauser, S., Adelmant, G., Troy, A.E., McKeon, C., Darlington, G.J., and Spiegelman, B.M. (1999b). Cross-regulation of C/EBP alpha and PPAR gamma controls the transcriptional pathway of adipogenesis and insulin sensitivity. Mol. Cell *3*, 151–158.

Yoshida, T., Sakane, N., Wakabayashi, Y., Umekawa, T., and Kondo, M. (1994). Anti-obesity and anti-diabetic effects of CL 316,243, a highly specific beta 3-adrenoceptor agonist, in yellow KK mice. Life Sci. *54*, 491–498.

Yubero, P., Manchado, C., Cassard-Doulcier, A.M., Mampel, T., Vinas, O., Iglesias, R., Giralt, M., and Villarroya, F. (1994). CCAAT/enhancer binding proteins alpha and beta are transcriptional activators of the brown fat uncoupling protein gene promoter. Biochem. Biophys. Res. Commun. *198*, 653–659.

Zimmet, P.Z., and Alberti, K.G. (1997). The changing face of macrovascular disease in non-insulin-dependent diabetes mellitus: an epidemic in progress. Lancet *350*, SI1–4.